ELSEVIER

Journal of Organometallic Chemistry 648 (2002) 270–279

Journal of Organometallic Chemistry

www.elsevier.com/locate/jorganchem

The effect of trimethylsilyl substituents on the ring-slippage of bis-indenyl-molybdenocene derivatives

Isabel S. Gonçalves [a,b], Paulo Ribeiro-Claro [a,c], Carlos C. Romão [b,*], Beatriz Royo [b], Zara M. Tavares [b]

[a] *Department of Chemistry, University of Aveiro, Campus de Santiago, 3810-193 Aveiro, Portugal*

[b] *Instituto de Tecnologia Química e Biológica da Universidade Nova de Lisboa, Quinta do Marquês, EAN, Apartado 127, 2781-901 Oeiras, Portugal*

[c] *Química-Física Molecular, Faculdade de Ciências e Tecnologia, Universidade de Coimbra, 3004-353 Coimbra, Portugal*

Received 4 October 2001; accepted 13 November 2001

Abstract

A group of new trimethylsilyl indenyl derivatives of molybdenum is reported, starting from the allyl compound TMSIndMo(η^3-C_3H_5)$(CO)_2$ [TMSInd = η^3-$SiMe_3C_9H_6$]. The novel allyl Mo(II) complex, which is synthesized by the reaction of Mo(η^3-C_3H_5)$(CO)_2(NCMe)_2Cl$ with Li(TMSInd) in THF, is the precursor to trimethylsilyl indenyl derivatives. Treatment of TMSIndMo(η^3-C_3H_5)$(CO)_2$ with HCl and addition of LiInd or LiTMSInd gives the ring-slipped complexes (η^5-TMSInd)Mo(η^3-Ind)$(CO)_2$ or (η^5-TMSInd)Mo(η^3-TMSInd)$(CO)_2$ in high yield. The presence of the trimethylsilyl substituent changes substantially the flexibility of the indenyl groups. These new substituted indenyl complexes were characterized by experimental techniques and ab initio calculations, and examined by cyclic voltammetry.

Keywords: Substituted indenyl complexes; Trimethylsilyl group; Ring slippage; Molybdenum; Molybdenocene; Ab initio calculations

1. Introduction

Following Basolo's discovery of the 'indenyl effect', in 1983, to signify the large rate differences found between similar substitution reactions undergone by [$CpML_n$] and [$IndML_n$] analogue complexes, (Cp = η^5-cyclopentadienyl; Ind = η^5-indenyl) [1], a significant number of studies were carried out aiming at understanding the bonding properties of the indenyl ligand and its ring slippage processes early reviewed by O'Connor and Casey [2]. Structural and spectroscopic studies on [$IndRhL_2$] complexes disclosed a systematic slip distortion of the η^5-Ind ring on the way towards a trihapto coordination, that is, with longer M–C bonds to the ring junction C atoms [3]. Although [(η^5-$C_9Me_7)_2Fe$] seems to be the least slip distorted indenyl complex yet structurally characterized [4], the presence of substituents on the indenyl ring does not necessarily cause a profound effect on the slip distortion of η^5-Ind containing complexes since [η^5-IndRh(η^4-1,5-C_8H_{12})] and [(η^5-C_9Me_7)Rh(η^4-1,5-C_8H_{12})] show similar slip distortion parameters [3]. The slip away from the centre of the C5 ring may be accompanied by a bending of the indenyl ring. This slip-fold distortion, first observed by Köhler in 1974 for [Ind_2Ni] [5] can actually be quite pronounced as shown crystallographically for the true 18e trihapto indenyl derivatives η^3-$IndIr(PPhMe_2)_3$ [6], and [η^3-$IndW(CO)_2(NCMe)_3$][BF_4] [7] but has very small values for the 18e slip-distorted [(η^5-Ind)ML_n] complexes [3]. ^{13}C-NMR studies on a large set of d^6 and d^8 $IndML_n$ complexes correlated the degree of bending with the deshielding of ^{13}C resonances of the ring junction carbon atoms [8].

When a 2e donor, L′, is added to an 18e complex [(η^5-Ind)ML_n], a ring-slipped species [(η^3-Ind)ML_nL'] may be formed as in the cases of both η^3-$IndIr(PPhMe_2)_3$ [6], and [η^3-$IndW(CO)_2(NCMe)_3$][BF_4] [7a]. However, few examples of this type of associative processes are known and a delicate dependence on the nature of L and L′ has been reported [7b]. Likewise, reduction of an 18e complex [(η^5-Ind)ML_n]$^{n+}$ by 2

* Corresponding author. Tel.: +351-21-44169751; fax: +351-21-441-1277.

E-mail address: ccr@itqb.unl.pt (C.C. Romão).

0022-328X/02/$ - see front matter
PII: S0022-328X(01)01479-6

electrons may induce the formation of a ring-slipped 18e species $[(\eta^3\text{-Ind})ML_n]^{((n+1)-2)}$. Relevant examples of this type of studies were carried out on $[(\eta^5\text{-Ind})Mn(CO)_3]$ [9a], $[(\eta^5\text{-Ind})Fe(CO)_3]^+$ [9b] and $[(\eta^5\text{-Ind})Rh(\eta^4\text{-1,5-}C_8H_{12})]$ [9c]. In all these cases, an important effort was devoted to the assignment of the hapticity of the intermediate radical product resulting from 1e reduction. A 19e species, therefore, with a η^5-Ind ring, was proposed for both the Mn and Fe cases, whereas a 17e species $[(\eta^3\text{-Ind})Rh(\eta^4\text{-1,5-}C_8H_{12})]^-$ seemed to be most likely for the Rh complex reduction. Similar ring slippages for the corresponding cyclopentadienyl complexes are more complex to interpret. Among other examples, they are not observed on reduction of $[CpFe(CO)_3]^+$ [9b]. $[(\eta^3\text{-MeCp})Mn(CO)_3]^{2-}$ is formed on reduction of the neutral parent complex [9d] and a 19e radical was identified on the reduction of $[CpM(CO)_2(NO)]^+$ (M = Mn, Re) [9e].

In most aspects of this kind of problems, bent metallocene derivatives of both Groups 5 and 6 have provided some of the most clearcut examples of ring slippage of cyclopentadienyl type ligands. From the earliest example of a de bona fide bent η^3-Cp ligand structurally characterized, in $(\eta^3\text{-Cp})CpW(CO)_2$ [10], to the ligand and redox induced indenyl slippage studies on $(Ind)_2V(CO)_2$ [11a,b] and chromocenes [11c,11d], and our series of studies on $[Ind(Cp')ML_2$ metallocenes (M = Mo, W); (Cp′ = Cp, Ind) [12], it became clear that these systems are able to provide a good insight into the factors that control such haptotropic shift processes. Reduction of $[Cp_2M(CO)_2]^{2+}$ readily forms $(\eta^3\text{-Cp})CpM(CO)_2$ (M = Mo, W). Redox induced ring slippages on the systems $[Ind(Cp)ML_2]^{2+} \rightarrow [(\eta\text{-Ind})(Cp)ML_2]^+ \rightarrow [(\eta^3\text{-Ind})CpML_2]$ allowed the characterization of the intermediate monocation by ESR spectroscopy. Its structure was calculated by DFT methods [13] showing that the redox induced $\eta^3 \rightarrow \eta^5$ slippage of the indenyl ring is a smooth process in as much as this intermediate presents a structure with bonding characteristics for the η-Ind ring that are intermediate between η^3 and η^5. As shown for the vanadocene and chromocene cases, ring slippage can also be achieved by ligand addition as in the formation of $Cp'_2Cr(CO)_2$ from $Cp'_2Cr(CO)$ under CO pressure (Cp′ = Cp, Cp*) [11a,11d,14]. The remarkably higher stability of $(\eta^3\text{-Cp*})(\eta^5\text{-Cp*})Cr(CO)_2$ relative to $Cp_2Cr(CO)_2$ points out the importance of substituent effects on the structural flexibility of the cyclopentadienyl ring. In fact, it has been recognized long ago that substituents at the Cp ring play a role in the ring-slippage motions of this ligand. Indeed, O_2NCp complexes react faster than their Cp counterparts in associative substitution processes [15] and Crabtree has even proposed a 'phenyl-Cp' effect based on his studies of the (PhCp)Ir complexes [16]. On the other hand, studies of the influence of substituents on the indenyl ring in this context are scarce [3b,4] and, to the best of our knowledge, not examined on bent η^3-IndML_n systems.

Following our studies on these processes the present paper addresses the study of the influence of a trimethylsilyl substituent upon the bending and slippage of the Me_3Si-indenyl ligand compared to its unsubstituted counterpart in $IndMo(\eta^3\text{-TMSInd})(CO)_2$ and $TMSIndMo(\eta^3\text{-TMSInd})(CO)_2$ complexes (TMSInd = Me_3SiInd). The trimethylsilyl group was chosen for its inductive effects which range from slightly more electron donating than a methyl group to more electron donating than a *tert*-butyl [17] and are therefore expected to substantially modify the flexibility of the indenyl groups.

2. Results and discussion

2.1. Chemical studies

A method of preparing differentially substituted metallocene complexes was developed using an allyl precursor of the type $Cp'M(\eta^3\text{-}C_3H_5)(CO)_2$ (Cp′ = Cp, CpR, Ind; M = Mo, W) which is conveniently available in excellent yield [12,18]. This method also applies for the synthesis of substituted indenyl analogues, and the allyl precursor, $TMSIndMo(\eta^3\text{-}C_3H_5)(CO)_2$ (**1**), is available from $Mo(\eta^3\text{-}C_3H_5)Cl(CO)_2(NCMe)_2$ and LiTMSInd in almost quantitative yield (Scheme 1). The IR spectrum shows the expected two very strong and somewhat broadened CO stretching vibrations. This broadening arises from the existence of two isomers with the *exo*- and *endo*-allyl conformations (see below), and this hypothesis is supported by the ^{1}H-NMR and ^{13}C-NMR spectra at room temperature. Two sets of signals are assignable to these isomers. We assign the *exo*-conformation to the more abundant isomer on the basis of the high field shift of the resonance of its *meso*-allylic proton δ (multiplet) 0.17–0.29 ppm compared with the normal value of δ (multiplet) 3.47–3.36 ppm found for the other isomer. The ring currents of the indenyl ligand are considered responsible for this shift and will more obviously affect the *exo*-isomer (A). A study of the NMR spectra of the fluxional unsubstituted analogue $IndM(\eta^3\text{-}C_3H_5)(CO)_2$ has reached the same conclusions [19].

The reaction of $TMSIndMo(\eta^3\text{-}C_3H_5)(CO)_2$ (**1**) with HCl in CH_2Cl_2 gives an intermediate pink–red powder, which dissolves in THF and reacts with LiInd or Li(TMSInd) at low temperature to afford high yields of $(\eta^5\text{-TMSInd})Mo(\eta^3\text{-Ind})(CO)_2$ (**2**) as a red solid or $(\eta^5\text{-TMSInd})Mo(\eta^3\text{-TMSInd})(CO)_2$ (**3**) as a red oil (Scheme 1).

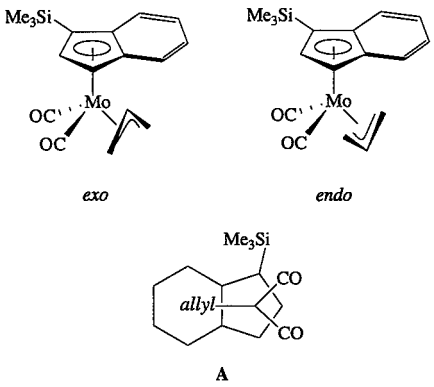

These complexes are extremely soluble in hexane or pentane compared to other related complexes of the type Cp′Mo(η^3-Ind)$(L)_2$ [12,20] and do not precipitate from the solution after concentration. They are air and moisture sensitive and must be handled and stored under moisture-free inert gas atmosphere. Unfortunately, suitable X-ray quality crystals of **2** could not be grown and complex **3** is oil. Therefore, the structural characterization of the complexes was mainly based on NMR evidence.

The most important aspect in the characterization of complex **2** concerns the establishing of the hapticities of each the indenyl rings. In fact, assuming an 18-electron count for complexes **2** and **3**, a rigid structure would have one η^5-indenyl and one η^3-indenyl. However, exchange may take place between them in solution as in the case of the complexes (η^5-Ind)M(η^3-Ind)$(CO)_2$ (M = Mo, W), that only present three signals with an intensity ratio of 4:2:1 in their ^{1}H-NMR spectra [12].

In order to assign the ring hapticities by NMR it is therefore necessary that exchange is slow or inexistent. One might expect that complex **3**, bearing bulky substituents on both indenyl rings would show no fluxionality and, therefore would allow the spectral assignment of the ^{1}H-NMR peaks for both η^5-TMSInd and η^3-TMSInd.

In fact, the ^{1}H-NMR for (η^5-TMSInd)Mo(η^3-TMSInd)$(CO)_2$ (**3**) reveals no fluxionality at room temperature. In agreement with two different hapticities for both indenyl rings, the ^{1}H-NMR spectrum of **3** presents two sets of TMSindenyl signals. The chemical shifts of the protons in the η^5-coordinated TMSindenyl follow the pattern exemplified in the case of **1**.

The resonances for the η^3-TMSindenyl appear as two multiplets at δ 6.80 and 6.55 ppm for the benzenoid protons, and two doublets at 6.96 and 5.18 which are difficult to assign individually to either H_{12} or H12. The low field shift of the benzenoid ring protons (H14–17) in going from η^5-TMSInd to η^3-TMSInd is typical and has been well documented before [7b]. The difference in chemical shifts observed for the H11 and/or H12 protons in both rings is expected in comparison to previous results. Typically, the H11 signal shifts up-field on going from η^5-coordination to η^3-coordination and is expected at ca. δ 5.3 ppm [7b]. However, the H11 proton (H2 in non-substituted indenyl rings) has a more unpredictable pattern of shifts upon ring-slippage rearrangements. In the general case of complexes bearing only one indenyl ring, it generally shifts down-field upon η^5 to η^3 ring slippage (Table 1) [7b]. In the case of systems with two indenyl rings H2 shifts up-field upon η^5 to η^3 ring slippage, as exemplified in (η^5-Ind)W(η^3-Ind)$(CO)_2$ (δ 3.4 ppm H2) [21] (Table 1). This low-field shift is certainly due to ring currents originating from the Ind$M(CO)_2$ fragment and may be

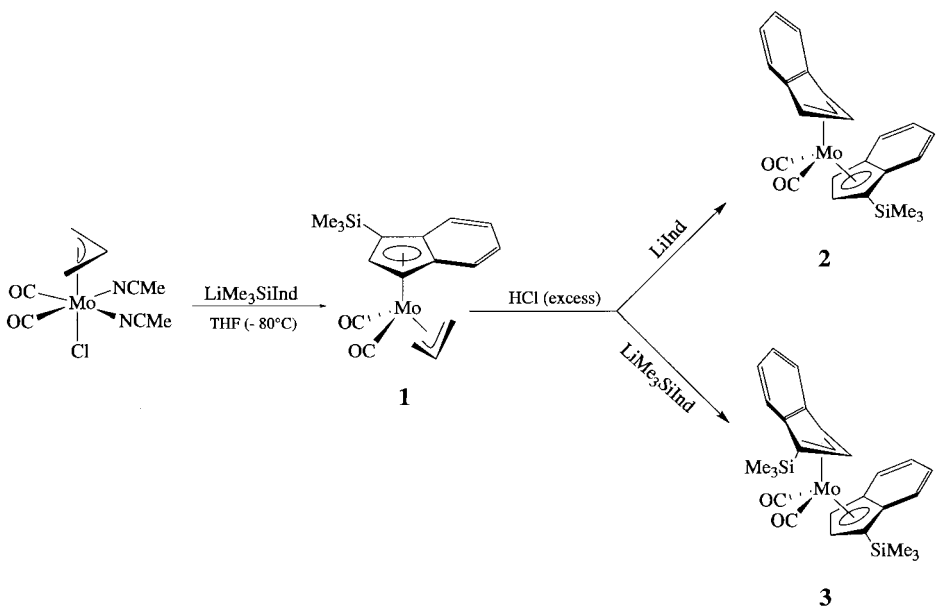

Scheme 1.

Table 1
Selected ^{1}H data for related compounds

Complex	References	η-Indenyl resonances (δ ppm)		
		H5/8	H1/3	H2
[(η^5-Ind)Mo(CO)$_2$-(NCMe)$_2$]BF$_4$	[12d]	7.60–7.54 m	6.07 d	5.02 t
[(η^3-Ind)Mo(CO)$_2$-(NCMe)$_3$]BF$_4$	[12d]	6.47–6.37 m	5.10 d	7.20 t
CpMo(η^3-Ind)(CO)$_2$	[12a]	6.67 m; 6.43 m	5.20 d	6.75 t
(η^5-Ind)Mo(η^3-Ind)-(CO)$_2$	[18a]	6.69–6.66 m	5.11 d	4.80 t
(η^5-Ind)W(η^3-Ind)-(CO)$_2$	[21]	6.6 m	4.8 d	3.40 t
(η^5-Ind)Mo(η^3-Ind)-{P(OMe)$_3$}$_2$	[18b]	6.88 m; 6.51 m	5.72 d	5.46 t

subject to unexpected changes upon small changes in the geometry of the molecule. Therefore, values like δ 5.4 ppm have been observed, for instance in Ind$_2$Mo{P(OMe)$_3$}$_2$ [18b]. These facts make the individual assignment of the signals H11 and H12 in complex **3** difficult to make although they both appear in expectable regions.

We may then conclude that molecule **3** is structurally rigid. According to the ab initio results (see below), this restriction of fluxionality relative to IndMo(η^3-Ind)(CO)$_2$ arises from the restriction of rotation imposed by the bulky SiMe$_3$ substituents in the TMSInd ligands.

In the ^{1}H-NMR spectrum of the mixed ring (η^5-TMSInd)Mo(η^3-Ind)(CO)$_2$ (**2**), at room temperature, only a slight broadening of the signals is observed indicating very slow exchange of the rings and an almost rigid structure. The resonances of the six-membered protons of both rings overlap partially in a complex pattern between ca. δ 7.61 and 6.68 ppm (H14–17 plus H5–8). However, in the region of the protons of the five-membered rings, there are clearly two sets of signals. The TMSInd ring shows two doublets at δ 5.89 and 5.17 ppm together with a singlet at 0.49 ppm attributed to the silyl substituent. Accordingly, the chemical shifts of the protons on the unsubstituted indenyl ring are consistent with η^3-coordination, these values are within the range of those measured in other trihapto bisindenyl complexes [12]. The η^3-coordination is also predicted, from ab initio calculations, to be more stable than the η^5-coordination, although by only 0.5 kJ mol^{-1}. (This value is above the margin of errors of the calculations below thermal energy at ambient temperature, which means that, in the absence of other effects, both forms would have appreciable population at room temperature.) The H1 and H3 protons appear as a doublet (somewhat broadened) at δ 4.21 ppm whereas the H2 proton appears as a *triplet* (somewhat broadened) at δ 3.42 ppm. This up-field shift is consistent with a η^3-Ind ligand in a bisindenyl system as pointed out above. These NMR results show that ring slippage is favoured for the unsubstituted ring and the structure of **2** in solution is (η^5-TMSInd)Mo(η^3-Ind)(CO)$_2$.

Further confirmation of the trihapto coordination of the indenyl ring in **2** and **3** stems from the large deshielding of the ring junction C4/9 carbon atoms in the ^{13}C-NMR spectra [8]. These types of values also indicate that the η^3-indenyl coordination in **2** and **3** is associated with a marked slip-fold distortion (Ω; see Ref. [22] for definition). When η^5 hapticity is present, the indenyl ligand is almost planar and a very small value for the Ω angle is expected. Values of ca. 120 ppm for these quaternary carbon atoms correspond to a typical η^5-indenyl coordination with a fold angle close to 0°, i.e. a planar indenyl ligand. In some cases an appreciable degree of bending is observed, e.g. [(η^5-Ind)Rh(μ-PPh$_2$)$_3$ZrCp$_2$] ($\Omega = 8.5°$; δ 127 ppm, C4/C9) [8].

Strongly bent rings give rise to C4/9 resonances at higher δ ppm values as exemplified by the isoelectronic CpMo(η^3-Ind)(CO)$_2$ ($\Omega = 26°$; δ 151.1 ppm, C4/9) [12b] or to other bent indenyls, e.g. [(η^5-Ind)Ir(PMe$_3$)$_3$] ($\Omega =$ 28°; δ 156.7 ppm, C4/C9) [6].

In the present case, the values of δ 144.59 ppm (C4/9) and δ 144.05 ppm (C13/18) for **2** and **3** suggest a large Ω, ca. 20°. Calculated values for folding angles of IndMo(η^3-Ind)(CO)$_2$, **2** and **3** range from a maximum value of 23.5° in the unsubstituted indenyl group of **2** to a minimum value of 19.5° in **3** (see below).

Given the similarity of structural and electronic features of complexes **2** and **3** with others of the general formula (η^5-Cp′)Mo(η^3-allyl)(CO)$_2$, comparison of the values of the ν(CO) stretching vibrations (Table 2) should be indicative of the relative electron richness of the metal centre which, in turn, reflects the relative donor capabilities of the several ligands involved. A rapid comparison of the ν(CO) values of the isostructural IndMo(η^3-C$_3$H$_5$)(CO)$_2$, (MeInd)Mo(η^3-C$_3$H$_5$)-(CO)$_2$ and (TMSInd)Mo(η^3-C$_3$H$_5$)(CO)$_2$, suggests the following decreasing order of donor ability: η^5-TMSInd > η^5-MeInd > η^5-Ind. This quite unexpected trend seems to be supported by the ab initio calculations. Comparing the optimized structures for IndMo(η^3-Ind)(CO)$_2$ and **3** (see below), while the C–O bond lengths are all quite similar, the Mo–CO distance shows a clear decrease consistent with the above mentioned donor ability. More convincing are the results from population analysis, as both Mulliken and natural bond orbitals (NBO) approaches clearly show that the electron transfer from the TMSInd fragment is higher than that from the Ind fragment. The NBO population analysis (more reliable than the simplistic Mullikan scheme) yields an average increase of ca. 38 me$^-$ charge donation from η^5-Ind to η^5-TMSInd. However, such trends are not reflected in the redox potentials of these complexes, as discussed below.

A well-known property imparted by alkyl or silyl substituents on Cp or Ind rings is the increase in solubility of the corresponding substituted complexes compared to the parent species. The chemistry of several dications, $[Ind_2MoL_2]^{2+}$ and $[IndCpMoL_2]^{2+}$, that we have prepared before has been limited precisely by this lack of solubility in non-coordinating solvents. We therefore decided to prepare the dicationic derivatives of the silylated bisindenyl complexes. Reaction of (TMSInd)Mo(η^3-Ind)$(CO)_2$ (**2**) with two equivalents of triphenylcarbenium tetrafluoroborate in dichloromethane at room temperature gives the dication [Ind(TMSInd)Mo$(CO)_2$][BF_4]$_2$ (**4**) which is soluble in dichloromethane but was not further characterized. As expected, the CO ligands are labile and dissolution of the complex in NCMe gives solvolysis producing [(TMSInd)IndMo(NCMe)(CO)]$^{2+}$ (**5**). This chiral-at-metal complex has a ^{1}H-NMR spectrum compatible with η^5-coordination of the indenyl ligands. The coordinated NCMe molecule displays in the ^{1}H-NMR spectrum a singlet at δ 2.19 ppm. So far we have not attempted to resolve the enantiomeric mixture of these potentially stereogenic centres.

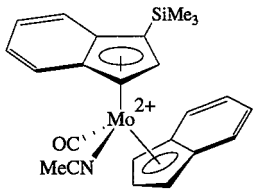

5

2.2. Ab initio calculations

Having determined the indenyl hapticities for **2** and **3** by ^{1}H-NMR spectroscopy, ab initio calculations were carried out to study these ring slippages and provide the optimized structures. These calculations have been performed for the compounds IndMo(η^3-Ind)$(CO)_2$, **2** and **3**, at the B3LYP/LanL2DZ level, considering several distinct starting geometries. The calculated molecular structures for the most relevant energy minima are

Table 2
Values for CO stretching vibrations of selected complexes

Compound	ν(CO) [a] (cm^{-1})	References
IndMo(η^3-C_3H_5)$(CO)_2$	1946, 1861 [b]	[12b]
MeIndMo(η^3-C_3H_5)$(CO)_2$	1944, 1859 [b]	[26]
TMSIndMo(η^3-C_3H_5)$(CO)_2$ (**1**)	1931, 1854	This work
IndMo(η^3-Ind)$(CO)_2$	1944, 1851	[18]
TMSIndMo(η^3-Ind)$(CO)_2$ (**2**)	1931, 1863	This work
TMSIndMo(η^3-TMSInd)$(CO)_2$ (**3**)	1922, 1827	This work

[a] Solid-state KBr IR spectra (ν_{sym}, ν_{asym}).
[b] Hexane solution.

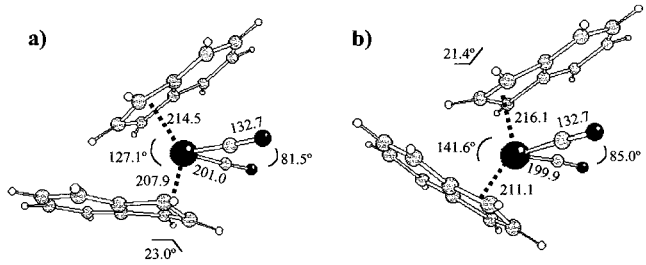

Fig. 1. Optimized geometries for the two lowest energy minima of IndMo(η^3-Ind)$(CO)_2$ at the B3LYP/LanL2DZ level. Only the most relevant parameters are shown. The absolute energy of form (a) is $-219.6477300E_h$.

in good agreement with the available X-ray and theoretical data, for the present system and similar ones [12a–c,23,24].

The IndMo(η^3-Ind)$(CO)_2$ system presents two minima, with a calculated energy difference of ca. 8 kJ mol^{-1}, shown in Fig. 1. The two structures differ in the relative orientations of the η^3/η^5-indenyl and carbonyl ligands. The higher energy form *in vacuum* is favoured in the crystal, and the structure of Fig. 1b is directly comparable with the reported X-ray data [12b]. As expected, the calculated bond lengths are systematically longer than the experimental ones. For instance, the calculated C–Mo distances for the η^5-coordinated indenyl group are in the range of 243–252 pm, while the corresponding X-ray values are in the range of 232–244 pm [12b]. In the case of the η^3-coordinated indenyl group, C–Mo distances for the three bonded carbon atoms are 228 and 250 pm (X-ray: 221 and 244 pm [12b]); the remaining two carbon atoms of the five-membered ring are away from the Mo atom by 323 pm (X-ray: 317 pm [12b]). Other bond length values, shown in Fig. 1b, display the same general behaviour. A good agreement is found for the values of bond angles, also compared in Fig. 1b. The folding angles Ω, often used to characterise the indenyl ligands, have the values 4 and 21.4° (calculated) and 3 and 20.8° (X-ray), for the η^5- and η^3-coordination, respectively. The calculated rotation angle λ, giving the relative orientation of the two indenyl groups (as defined in [12b]) is 180°, corresponding to a Cs symmetry, and is comparable to the experimental value $\lambda = 179.3°$ [12b].

The calculated structures for the systems **2** and **3** are shown in Figs. 2 and 3, respectively. Only the most relevant molecular parameters (coordination distances and angles, Ω and λ angles) are shown for simplicity. To the best of our knowledge, there are no previous structural studies of $SiMe_3$-indenyl ligands. Nonetheless, the structures reported herein compare with both theoretical and experimental studies of related indenyl complexes [12a–c,23].

Two close minima were found for **2**, with an energy difference of only ca. 0.5 kJ mol^{-1}. The structure of the

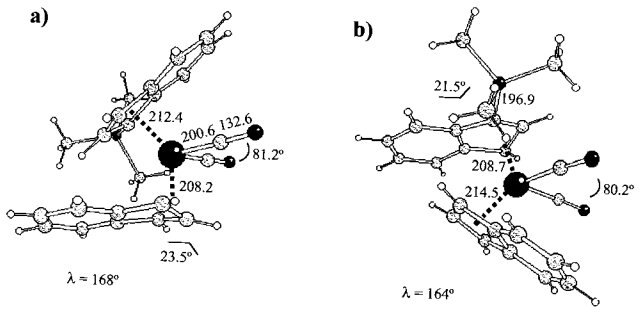

Fig. 2. Optimized geometries for the two lowest energy minima of **2** at the B3LYP/LanL2DZ level. Only the most relevant parameters are shown. The absolute energy of form (a) is $-245.2304470E_h$.

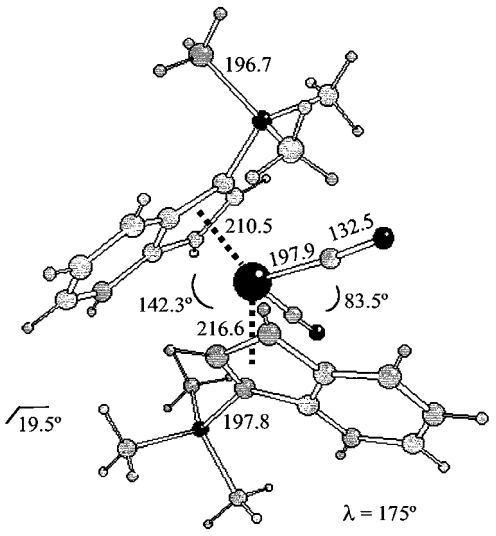

Fig. 3. Optimized geometry for the lowest energy minimum of **3** at the B3LYP/LanL2DZ level. Only the most relevant parameters are shown. The absolute energy of this form is $-270.8095954E_h$.

lowest energy form (Fig. 2a) is in agreement with the NMR solution data, but the absence of a second form in solution, may arise from other effects.

The comparison of the structures in Figs. 1–3 allows the evaluation of some interesting trends. Both the OC–Mo–CO bond angle and the λ orientation angle reach their lowest values in **2**, an effect easily related with the geometry distortion caused by a single $SiMe_3$ substituent. The folding angle Ω for the η^3-coordination also deserves some attention, as it shows a decrease from the unsubstituted indenyl to the ($SiMe_3$)-indenyl ligands. This trend is followed by an increase of the Mo–C distances and seems to correlate with the bonding strength of the η^3-Ind ligand.

2.3. Electrochemical studies

Relevant electrochemical data for complexes **1**–**3** as well as a few other related complexes were obtained in NCMe and CH_2Cl_2 (containing 0.1 M tetrabutylammonium hexafluorophosphate) and are summarized in Table 3. Only minor variations of the peak potentials were registered indicating that no solvent dependent processes are present.

The cyclic voltammogram (CV) of complex (TMSInd)Mo(η^3-C_3H_5)$(CO)_2$ (**1**) shows an oxidation at 0.73 V versus SCE and three reductions at 0.18, −0.23, and −0.97 V. This result is comparable with other similar allylic complexes of the type CpMo(η^3-C_5H_7)L_2 [25]. The indenyl complexes Ind′Mo(η^3-C_3H_5)$(CO)_2$ (Ind′ = Ind, MeInd) present the same behaviour but the parent allylic complex CpMo(η^3-C_3H_5)$(CO)_2$ undergoes a reversible oxidation [25].

A more interesting situation is found in the cyclic voltammograms of the bisindenyl complexes, IndMo(η^3-Ind)$(CO)_2$, (TMSInd)Mo(η^3-Ind)$(CO)_2$ (**2**) and (TMSInd)Mo(η^3-TMSInd)$(CO)_2$ (**3**). Each of these complexes exhibits one two-electron reversible wave (Table 3, Fig. 4) that can be attributed to the two consecutive oxidations from Mo(II) to Mo(IV) accompanied by change of the hapticity (η^3-Ind′)(η^5-Ind′)$Mo(CO)_2 \rightarrow (\eta^5\text{-Ind}')(\eta^5\text{-Ind}')Mo(CO)_2]^{2+}$. The potential at which the electrochemical transformations take place is not significantly affected by the silylated substituent on the indenyl ring. To try to explain this, the HOMO energies for the three compounds IndMo(η^3-Ind)$(CO)_2$, **2** and **3** were calculated. The

Table 3
Cyclovoltammetric data for dicarbonyl complexes recorded in NCMe

Complexes	E_{pa} (V) [a]	E_{pc} (V) [b]	Comment
$Me_3SiIndMo(\eta^3\text{-}C_3H_5)(CO)_2$ (**1**)	0.73	–	–
	–	0.18	–
	–	−0.23	–
	–	−0.97	–
MeIndMo(η^3-C_3H_5)$(CO)_2$ [c]	0.66	–	–
	–	0.06	–
	–	−1.09	–
IndMo(η^3-C_3H_5)$(CO)_2$ [c]	0.69	–	–
	–	0.11	–
	–	−1.10	–
CpMo(η^3-C_3H_5)$(CO)_2$ [d]	0.60	0.55	rev
	–	−0.07	–
	–	−0.22	–
	–	−0.90	–
$Me_3SiIndMo(\eta^3\text{-Ind})(CO)_2$ (**2**)	0.22	0.26	rev
IndMo(η^3-Ind)$(CO)_2$	0.22	0.18	rev
CpMo(η^3-Ind)$(CO)_2^c$	0.19	0.12	irr
	–	−0.26	–
	–	−0.90	–
$Me_3SiIndMo(\eta^3\text{-}Me_3SiInd)(CO)_2$ (**3**)	0.21	0.26	rev

qr = quasi-reversible, irr = irreversible, rev = reversible.
[a] E_{pa}—Anodic sweep (peak potentials, Volts).
[b] E_{pc}—Cathodic sweep (peak potentials, Volts).
[c] See Ref. [26].
[d] See Ref. [25].

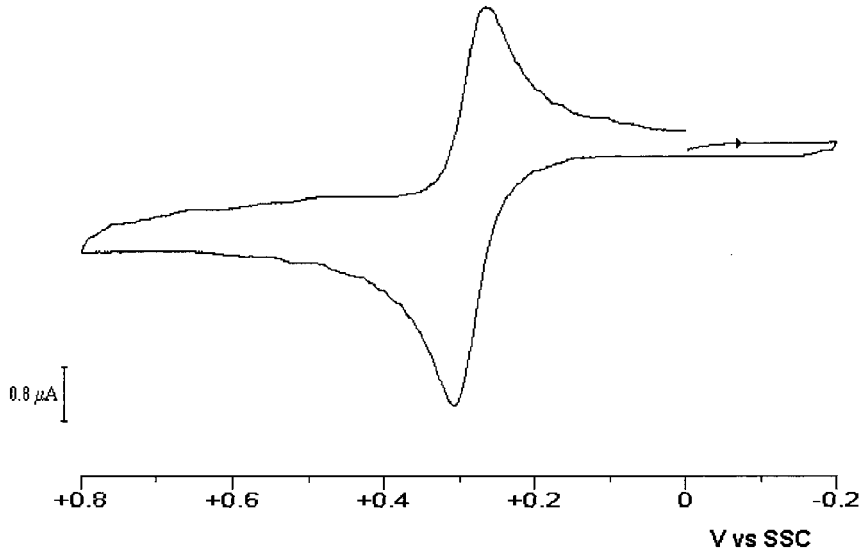

Fig. 4. Cyclic voltammogram of TMSIndMo(η^3-TMSInd)$(CO)_2$ (**3**) in NCMe/0.1 M $[NBu_4][PF_6]$ at 298 K; scan rate, 0.25 V s^{-1}.

values obtained (6.35, 6.18 and 6.02 eV, respectively) show a decrease on going from IndMo(η^3-Ind)$(CO)_2$ to **3**, but the magnitude of these changes is probably not sufficient to result in a clear trend in the corresponding oxidation potentials. Other related complexes have also shown the same lack of response to inductive effects, e.g. $[(\eta^5\text{-Ind})(\eta^5\text{-Cp})Mo(Bipy)]^{2+}$ ($E_{pa} = -0.59$ V) and $[(\eta^5\text{-Ind})(\eta^5\text{-Cp})Mo(^tBubipy)]^{2+}$ ($E_{pa} = -0.60$ V) [20].

These results for the three complexes contrast with that reported for the mixed-ring complex CpMo(η^3-Ind)$(CO)_2$ which shows an irreversible oxidation at 0.19 V versus SCE with a small cathodic response at 0.12 V, and two irreversible reduction waves at -0.26 and -092 V (also in NCMe). This irreversibility is due to rapid solvolysis of the dication $[IndCpMo(CO)_2]^{2+}$ to give $[IndCpMo(CO)(NCMe)]^{2+}$. When this solvolysis is slower or absent, as in the case of the tungsten analogue CpW(η^3-Ind)$(CO)_2$ [26], or in the case of the dications $[IndCpMoL_2][BF_4]_2$ (L = bipy, $^tBu_2$bipy, dppe, $P(OMe)_3$, etc.), two consecutive reductions accompanied by indenyl-slippage are also observed [20]. A thorough study of the systems with L = $P(OMe)_3$ and L_2 = dppe has been completed [13].

The redox and structural flexibility of the bisindenyl complexes, namely **2** and **3**, allied with the high solubility of their dicationic derivatives, **4** and **5**, prompts the study of the CO activation reactions in these molecules currently under way in our laboratory.

3. Conclusions

New molybdenocene analogues bearing silyl-substituted indenyl rings were prepared and characterized by NMR and cyclic voltammetry. In contrast to $Ind_2Mo(CO)_2$ which shows exchange of hapticity between both rings, the presence of the bulky Me_3Si substituent in the ring prevents the exchange of the indenyl ligands, each of them retaining its own type of hapticity. In the mixed ring case, the unsubstituted indenyl assumes η^3-coordination whereas the substituted one, TMSInd, remains η^5-coordinated. The presence of the TMS substituents is not felt in the values of the redox potentials measured by CV. In an attempt to shed some light on the role of steric and electronic factors on the structural preferences of the bisindenyl complexes, the experimental data has been combined with ab initio calculations. This set of results suggests that the conformation adopted by the TMS-indenyl ligand is determined, case to case, by a delicate balance between steric and electronic effects.

4. Experimental

4.1. Materials and procedures

All operations were carried out under an atmosphere of N_2 with standard Schlenk-line and glovebox techniques. Solvents were purified by conventional methods and distilled under N_2 prior to use. ^{1}H- and ^{13}C-NMR spectra were measured in a Bruker AMX 300 spectrometer. ^{1}H and ^{13}C chemical shifts are reported on the scale relative to Me_4Si (δ 0.0). IR spectra were measured in a Unicam Mattson model 7000 FTIR spectrometer using KBr pellets. Microanalyses and cyclic voltammetric measurements were performed in our laboratories (ITQB).

The electrochemical instrumentation consisted of a BAS CV–50 W–1000 Voltammetric Analyzer connected to BAS/Windows data acquisition software.

All the electrochemical experiments were run under Ar at room temperature (r.t.). Tetrabutylammonium hexafluorophosphate (Aldrich) was used as supporting electrolyte, and it was recrystallized from EtOH. Cyclic voltammetry experiments were performed in a glass cell MF-1082 from BAS in a C-2 cell enclosed in a Faraday cage. The reference electrode was SSC (MF-2063 from BAS) and its potential was −44 mV relative to an SCE.

The reference electrode was calibrated with a solution of ferrocene (1 mM) to obtain a potential in agreement with the literature value [27]. The electrochemical experiments on each complex were followed by addition of ferrocene to the solution, and a new cyclic voltammogram was recorded. The electrochemical behaviour of the complexes did not seem to be affected by the presence of ferrocene and vice versa.

The auxiliary electrode was a 7.5 cm platinum wire (MW-1032 from BAS) with a gold-plated connector. The working electrode was a platinum disk (MF-2013 from BAS) with ca. 0.022 cm^2 sealed in Kel-F plastic. Between each CV scan the working electrode was electro-cleaned, polished on diamond 1 μM and alumina cleaning with water–MeOH and sonicated before use, according to standard procedures.

Solvents were dried and the solutions were degassed with dry N_2 (or Ar) before each experiment and an inert atmosphere was maintained over the solution.

$Mo(\eta^3\text{-}C_3H_5)(CO)_2(NCMe)_2Cl$ [28], Ph_3CBF_4 [29], Li(TMSInd) [30], and LiInd [18], were prepared as published.

4.2. Preparation of $TMSIndMo(\eta^3\text{-}C_3H_5)(CO)_2$ (1)

A mixture of solid Li(TMSInd) (1.87 g; 9.6 mmol) and $Mo(\eta^3\text{-}C_3H_5)(CO)_2(NCMe)_2Cl$ (3.00 g; 9.6 mmol) was weighed in a glove box and later placed in a Schlenk tube in a cold bath at −80 °C. Pre-cooled THF was added slowly and the temperature raised slowly to r.t. After 18 h total reaction time the mixture was taken to dryness and the residue extracted with hexane. Concentration of the yellow solution gave a yellow microcrystalline powder. Yield: 89%. Calc. for $C_{17}H_{20}MoO_2Si$ (404.39): C, 56.43; H, 4.99. Found: C, 56.33; H, 4.81%. IR (KBr, cm^{-1}): $\nu = 3048$ (m), 2959 (m), 2915 (m), 1931 (vs), ν(C≡O), 1854 (vs), ν(C≡O), 1402 (m), 1339 (m), 1248 (s), 1140 (m), 1043 (m), 960 (m), 839 (s), 822 (s), 748 (s), 694 (m), 613 (m), 582 (m), 530 (m). ^{1}H-NMR ($CDCl_3$, 300 MHz, r.t., ppm): $\delta =$ *Exo* 7.13–6.95 (m, 4H, H14–17), 6.13 (d, 1H, H11/12), 5.50 (d, 1H, H11/12), 2.34–2.26 (m, 2H, *syn*-C_3H_5), 0.98–0.86 (m, 2H, *anti*-C_3H_5), 0.45 (s, 9H, $Si(CH_3)_3$), 0.17–0.29 (m, 1H, *meso*-C_3H_5). *Endo* 7.13–6.95 (m, 4H, H14–17), 6.02 (d, 1H, H11/12), 5.45 (d, 1H, H11/12), 3.47–3.36 (m, 3H, *meso*- and *syn*-C_3H_5), −0.51, −1.25 (2 × d, 2 × 1H, *anti*-C_3H_5). $^{13}C\{^1H\}$-NMR ($CDCl_3$, 75 MHz, r.t., ppm): $\delta = 238.18$, 237.97 (CO), 124.90, 124.69, 124.55, 124.49, 124.41, 123.78 (C14–17), 117.05, 114.84 (C18/13), 93.53, 92.72 (C11/12), 83.63, 83.49 (C11/12), 80.68, 80.15 (C10), 55.15, 55.01 (C_2), 49.58, 48.95 ($C_{1/3}$), 1.00, 0.19 ($Si(CH_3)_3$).

4.3. Preparation of $TMSIndMo(\eta^3\text{-}Ind)(CO)_2$ (2)

Gaseous HCl was bubbled through a solution of $TMSIndMo(\eta^3\text{-}C_3H_5)(CO)_2$ (0.72 g, 1.79 mmol) in CH_2Cl_2 (20 ml) for 2 min and the mixture was stirred for a further 8 h to complete the reaction. The pink–red solution was evaporated, washed with hexane, and dried under vacuum. A mixture of LiInd (0.22 g, 1.79 mmol) and the resulting residue was placed in a cold bath at −60 °C. Pre-cooled THF was added and the temperature slowly raised to r.t. After 10 h, the mixture was taken to dryness and the residue extracted with hexane. The solution obtained was concentrated to dryness to yield compound **2**. Yield: 90%. Calc. for $C_{23}H_{22}MoO_2Si$ (454.45): C, 60.79; H, 4.88. Found: C, 60.65; H, 4.72%. IR (KBr, cm^{-1}): $\nu = 3075$ (m), 2955 (m), 1931 (vs) ν(C≡O), 1863 (vs) ν(C≡O), 1450 (m), 1402 (m), 1379 (m), 1385 (m), 1288 (m), 1252 (s), 1143 (m), 1043 (m), 960 (m), 837 (s), 819 (m), 758 (m), 746 (s), 694 (m), 599 (m), 563 (m), 532 (m). ^{1}H-NMR (CD_2Cl_2, 300 MHz, r.t., ppm): $\delta = 7.61$–6.68 (m, 8H, H14–17 and H5–8), 5.89 (d, 1H, H11/12), 5.17 (d, 1H, H11/12), 4.21 (d, 2H, H1 and H3), 3.42 (t(br), 1H, H2), 0.49 (s, 9H, $Si(CH_3)_3$). $^{13}C\{^1H\}$-NMR ($CDCl_3$, 75 MHz, r.t., ppm): $\delta = 200.98$, 144.59 (C9/4), 136.67, 132.05, 130.74, 128.45, 128.20, 126.61, 124.63, 122.73, 122.62, 121.02, 94.75, 81.26, 50.64, 46.45, −1.18 ($Si(CH_3)_3$).

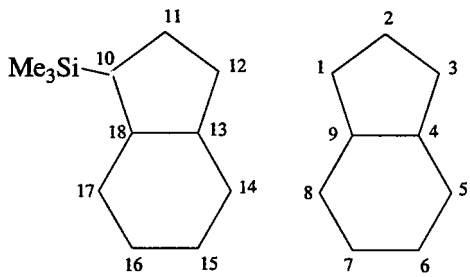

4.4. Preparation of $TMSIndMo(\eta^3\text{-}TMSInd)(CO)_2$ (3)

Gaseous HCl was bubbled through a solution of $TMSIndMo(\eta^3\text{-}C_3H_5)(CO)_2$ (0.64 g, 1.59 mmol) in CH_2Cl_2 (20 ml) for 2 min and the mixture was stirred for a further 8 h to complete the reaction. The pink–red solution was evaporated, washed with hexane, and dried under vacuum. A mixture of LiTMSInd (0.31 g, 1.59 mmol) and the resulting residue was placed in a cold bath at −70 °C. Pre-cooled THF was added and the temperature slowly raised to r.t. After 12 h, the mixture was taken to dryness and the residue extracted

with hexane. The solution obtained was concentrated to dryness to yield compound **3** as a dark-red oil. Yield: 88%. Calc. for $C_{26}H_{30}MoO_2Si_2$ (526.64): C, 59.30; H, 5.74. Found: C, 59.26; H, 5.45%. IR (KBr, cm^{-1}): $\nu = 3067$ (m), 2955 (s), 1923 (vs) ν(C≡O), 1827 (vs) ν(C≡O), 1461 (m), 1402 (m), 1379 (m), 1385 (m), 1288 (m), 1251(s), 1143 (m), 1019 (m), 960 (m), 837 (s), 839 (m), 766 (m), 718 (s), 693 (m), 596 (m), 560 (m), 534 (m). ^{1}H-NMR ($CDCl_3$, 300 MHz, r.t., ppm): $\delta = 7.53$–7.22 (m, 4H, H14–17), 6.96 (br, 1H, H11/12), 6.70–6.66 (m, 2H, H14–17), 6.63 (br, 1H, H11/12), 6.61–6.49 (m, 2H, H14–17), 5.38 (br, 1H, H11/12), 5.18 (d, 1H, H11/12), 0.41 (s, 9H, $Si(CH_3)_3$), 0.15 (s, 9H, $Si(CH_3)_3$). $^{13}C\{^1H\}$-NMR ($CDCl_3$, 75 MHz, r.t., δ ppm): 206.36, 144.05 (C13/18), 128.78, 125.49, 124.98, 123.52, 122.60, 120.91, 125.89, 100.48, 87.75, 79.24, 55.7, −1.27, −1.51 ($Si(CH_3)_3$).

4.5. Preparation of [(TMSInd)IndMo(CO)(NCMe)][BF_4]$_2$ (5)

A solution of [(TMSInd)IndMo(CO)$_2$][BF_4]$_2$ (0.50 mmol) in MeCN (20 ml) was stirred for 10 min at r.t. After concentration of the resulting yellow solution to 5 ml and addition of Et_2O, a yellow crystalline precipitate was obtained. The solid was filtered off, washed with hexane and dried under vacuum. Yield: 96%. Calc. for $C_{25}H_{25}MoOSiNB_2F_8$(653.12): C, 45.98; H, 3.86; N, 2.12. Found: C, 45.76; H, 3.83; N, 2.30%. Selected IR (KBr, cm^{-1}): $\nu = 2053$ (vs) ν(C≡O), 2325, 2289 (w) ν(N≡C). ^{1}H-NMR ($NCCD_3$, 300 MHz, r.t., ppm): $\delta =$ 7.73–7.18 (m, 8H, H14–17 and H5–8), 6.93 (d, 2H, H1/3), 6.03 (t, 1H, H2), 5.82 (d, 1H, H11/12), 5.48 (d, 1H, H11/12), 2.19 (s, 3H, Me), 0.28 (s, 9H, $Si(CH_3)_3$).

4.6. Ab initio calculations

Ab initio calculations were performed using the G98W program package [31] running on a personal computer (Pentium 830 MHz, 320 MB RAM). The geometry of several possible structures was fully optimized at the B3LYP level using the Dunning/Huzinaga valence double-zeta basis set for the first period elements [32], and the Los Alamos Effective Core Potentials plus double-zeta [33] for the Mo atom (LanL2DZ option of G98). This approach (B3LYP/LanL2DZ) has proven to yield a good quality/computational cost ratio for transition metal complexes and organometallics [24,34]. Natural Population Analysis was carried out using NBO program [35] as implemented in G98.

Acknowledgements

This work was supported by PRAXIS XXI under project 2/2.1/QUI/316/94 and under project POCTI/36127/QUI/2000. B. Royo (BPD) thanks FCT for grant.

References

[1] M.E. Rerek, L.-N. Ji, F. Basolo, J. Chem. Soc. Chem. Commun. (1983) 1208.
[2] J.M. O'Connor, C.P. Casey, Chem. Rev. 87 (1987) 307.
[3] (a) A.K. Kakkar, S.F. Jones, N.J. Taylor, S. Collins, T.B. Marder, J. Chem. Soc. Chem. Commun. (1989) 1454;
(b) T.M. Frankcom, J.C. Green, A. Nagy, A.K. Kakkar, T.B. Marder, Organometallics 12 (1993) 3688 (and references therein);
(c) L.F. Veiros, Organometallics 19 (2000) 3127 (and references therein).
[4] S.A. Westcott, A.K. Kakkar, G. Stringer, N.J. Taylor, T.B. Marder, J. Organomet. Chem. 394 (1990) 777.
[5] F.H. Köhler, Chem. Ber. 107 (1974) 570.
[6] J.S. Merola, R.T. Kacmarcik, D. Van Engen, J. Am. Chem. Soc. 108 (1986) 329.
[7] (a) J.R. Ascenso, I.S. Gonçalves, E. Herdtweck, C.C. Romão, J. Organomet. Chem. 508 (1996) 169;
(b) M.J. Calhorda, C.A. Gamelas, I.S. Gonçalves, E. Herdtweck, C.C. Romão, L.F. Veiros, Organometallics 17 (1998) 2597.
[8] R.T. Baker, T.H. Tulip, Organometallics 5 (1986) 839.
[9] (a) S. Lee, S.R. Lovelace, N.J. Cooper, Organometallics 14 (1995) 1974;
(b) K.A. Pevear, M.M.B. Holl, G.B. Carpenter, A.L. Rieger, P.H. Rieger, D.A. Sweigart, Organometallics 14 (1995) 512;
(c) C. Amatore, A. Ceccon, S. Santi, J.-N. Verpeaux, Chem. Eur. J. 3 (1997) 279;
(d) S. Lee, N.J. Cooper, J. Am. Chem. Soc. 113 (1991) 716;
(e) Y. Huang, C.C. Neto, K.A. Pevear, M.M.B. Holl, D.A. Sweigart, Y.K. Chung, Inorg. Chim. Acta 226 (1994) 53.
[10] G. Huttner, H.H. Brintzinger, L.G. Bell, P. Friedrich, V. Benjenke, D. Neugebauer, J. Organomet. Chem. 145 (1978) 329.
[11] (a) R.M. Kowalewski, A.L. Rheingold, W.C. Trogler, F. Basolo, J. Am. Chem. Soc. 108 (1986) 2460;
(b) G.A. Miller, M.J. Therien, W.C. Trogler, J. Organomet. Chem. 383 (1990) 271;
(c) E.U. van Raaij, S. Mönkeberg, H. Kiesele, H.-H. Brintzinger, J. Organomet. Chem. 356 (1988) 307;
(d) E.U. van Raaij, H.H. Brintzinger, J. Organomet. Chem. 356 (1988) 315.
[12] (a) J.R. Ascenso, C.G. Azevedo, I.S. Gonçalves, E. Herdtweck, D.S. Moreno, C.C. Romão, J. Zühlke, Organometallics 13 (1994) 429;
(b) J.R. Ascenso, C.G. de Azevedo, I.S. Gonçalves, E. Herdtweck, D.S. Moreno, M. Pessanha, C.C. Romão, Organometallics 14 (1995) 3901 (and references therein);
(c) I.S. Gonçalves, C.C. Romão, J. Organomet. Chem. 486 (1995) 155;
(d) M.J. Calhorda, C.A. Gamelas, I.S. Gonçalves, E. Herdtweck, C.C. Romão, L.F. Veiros, Organometallics 18 (1999) 507.
[13] M.E. Stoll, P. Belanzoni, M.J. Calhorda, M.G.B. Drew, V. Félix, W.E. Geiger, C.A. Gamelas, I.S. Gonçalves, C.C. Romão, L.F. Veiros, J. Am. Chem. Soc. 123 (2001) 10595.
[14] E.U. van Raaij, H.H. Brintzinger, L. Zsolnai, G. Huttner, Z. anorg. allg. Chem. 577 (1989) 217.
[15] M.E. Rerek, F. Basolo, J. Am. Chem. Soc. 106 (1984) 5908.
[16] A. Habib, R.S. Tanke, E.M. Holt, R.H. Crabtree, Organometallics 8 (1989) 1225.
[17] (a) P.G. Gassman, P.A. Deck, C.H. Winter, D.A. Dobbs, D.H. Cao, Organometallics 11 (1992) 959;
(b) B.E. Bursten, M.R. Callstrom, C.A. Jolly, L.A. Paquette, M.R. Sivik, R.S. Tucher, C.A. Wartchow, Organometallics 13 (1994) 127.

[18] (a) M.G.B. Drew, V. Félix, I.S. Gonçalves, C.C. Romão, B. Royo, Organometallics 17 (1998) 5782;
(b) M.G.B. Drew, V. Félix, C.C. Romão, B. Royo, J. Chem. Soc. Dalton Trans. (2002) (in press).
[19] J.W. Faller, C.C. Chen, M.J. Mattina, A. Jakubowski, J. Organomet. Chem. 52 (1973) 361.
[20] C.A. Gamelas, E. Herdtweck, J.P. Lopes, C.C. Romão, Organometallics 18 (1999) 506.
[21] A.N. Nesmeyanov, N.A. Ustynyuk, L.G. Makarova, V.G. Andrianov, Yu.T. Struchkov, S.J. Andrae, Yu.A. Ustynyuk, S.G. Malyugina, J. Organomet. Chem. 159 (1978) 189.
[22] J.W. Faller, R.H. Crabtree, A. Habib, Organometallics 4 (1985) 929.
[23] M.J. Calhorda, C.A. Gamelas, C.C. Romão, L.F. Veiros, Eur. J. Inorg. Chem. (2000) 331.
[24] L. Veiros, Organometallics 19 (2000) 5557.
[25] C.G. de Azevedo, M.J. Calhorda, M.A.A.F. de C.T. de Carrondo, A.R. Dias, M.T. Duarte, A.M. Galvão, C.A. Gamelas, I.S. Gonçalves, F.M. da Piedade, C.C. Romão, J. Organomet. Chem. 544 (1997) 257.
[26] I.S. Gonçalves, PhD Dissertation, Technical University of Lisbon, 1996.
[27] I.V. Nelson, R.T. Iwamoto, Anal. Chem. 35 (1963) 867.
[28] R.G. Hayter, J. Organomet. Chem. 13 (1968) P_1.
[29] G.A. Olah, J.J. Svoboda, J.A. Olah, Synthesis (1972) 554.
[30] (a) L. Cedheim, L. Eberson, Synthesis (1973) 159;
(b) L. Meurling, Acta Chem. Scand. B 28 (1974) 295.
[31] M.J. Frisch, G.W. Trucks, H.B. Schlegel, G.E. Scuseria, M.A. Robb, J.R. Cheeseman, V.G. Zakrzewski, J.A. Montgomery, R.E. Stratmann, J.C. Burant, S. Dapprich, J.M. Millam, A.D. Daniels, K.N. Kudin, M.C. Strain, O. Farkas, J. Tomasi, V. Barone, M. Cossi, R. Cammi, B. Mennucci, C. Pomelli, C. Adamo, S. Clifford, J. Ochterski, G.A. Petersson, P.Y. Ayala, Q. Cui, K. Morokuma, D.K. Malick, A.D. Rabuck, K. Raghavachari, J.B. Foresman, J. Cioslowski, J.V. Ortiz, B.B. Stefanov, G. Liu, A. Liashenko, P. Piskorz, I. Komaromi, R. Gomperts, R.L. Martin, D.J. Fox, T. Keith, M.A. Al-Laham, C.Y. Peng, A. Nanayakkara, C. Gonzalez, M. Challacombe, P.M.W. Gill, B.G. Johnson, W. Chen, M.W. Wong, J.L. Andres, M. Head-Gordon, E.S. Replogle, J.A. Pople, GAUSSIAN 98 (Revision A.1), Gaussian, Inc., Pittsburgh PA, 1998.
[32] T.H. Dunning Jr., P.J. Hay, in: H.F. Schaefer (Ed.), Modern Theoretical Chemistry, vol. 3, Plenum, New York, 1976, p. 1.
[33] W.R. Wadt, P.J. Hay, J. Chem. Phys. 82 (1985) 284.
[34] (a) M. Siodmiak, G. Frenking, A. Korkin, J. Phys. Chem. A 104 (2000) 1186;
(b) V. Jonas, G. Frenking, M.T. Reetz, J. Comput. Chem. 13 (1992) 935;
(c) A.M. Amado, P.J.A. Ribeiro-Claro, J. Mol. Struct. (THEOCHEM) 469 (1999) 191.
[35] E.D. Glendening, A.E. Reed, J.E. Carpenter, F. Weinhold, NBO Version 3.1.